






Preventing environmental and health problems due to LPG transport tank leaks: fatigue and crack behavior of heat-treated steel investigation

Hendri Chandra^a , Muhammad Imam Ammarullah^{b,c,d} , M. Marwani^a , E. Ellyanie^a, W. Warizal^e, Dimas Aditya^a, Diah Kusuma Pratiwi^a  and Nurhabibah Paramitha Eka Utami^a 

^aDepartment of Mechanical Engineering, Faculty of Engineering, Universitas Sriwijaya, Indralaya, South Sumatera, Indonesia;

^bDepartment of Mechanical Engineering, Faculty of Engineering, Universitas Diponegoro, Semarang, Central Java, Indonesia;

^cUndip Biomechanics Engineering and Research Centre (UBM-ERC), Universitas Diponegoro, Semarang, Central Java, Indonesia;

^dDepartment of Mechanics and Aerospace Engineering, College of Engineering, Southern University of Science and Technology, Shenzhen, Guangdong, China; ^eUniversitas Djuanda, Bogor, West Java, Indonesia

ABSTRACT

This study aims to investigate the effects of welding on the fatigue and crack behavior of ASTM A36 steel, a low-carbon steel commonly used in various applications, particularly in pressure vessel transport tanks for preventing environmental and health problems due to liquid petroleum gas (LPG) transport tank leaks. This research evaluates the influence of welding on the material's properties through various testing methodologies, including impact and fatigue tests. The impact tests were conducted using the Charpy V-Notch method, while fatigue tests employed the repeated bending method. The specimens were subjected to testing at different temperatures and angles to evaluate their performance under various conditions. The findings indicate that welding introduces weaknesses in the material, affecting its impact energy and fatigue life. Visual observations and metallographic examinations further revealed the fracture characteristics and microstructural changes in welded and non-welded specimens.

ARTICLE HISTORY

Received 28 July 2023

Revised 19 November 2023

Accepted 8 January 2024

KEYWORDS

Fatigue; crack; pressure vessel; welding; fracture

REVIEW EDITOR

D T Pham d.t.pham@bham.ac.uk; phammec@gmail.com
Editor-in-Chief

CLASSIFICATION

Engineering & technology;
mechanical engineering
design; testing

1. Introduction

ASTM A36 is a type of low-carbon steel that processes attributes, such as strength, weldability and the ability to be machined. Low-carbon steel is characterized by its high ductility and susceptibility to corrosion, but it tends to have lower hardness and wear resistance (Kim et al., 2020; Pratiwi et al., 2023; Tamlichia et al., 2022; Utami & Chandra, 2017). To enhance its corrosion resistance, this steel can be electroplated or coated. Its usage in steel applications varies based on factors like thickness and the required level of corrosion resistance. Numerous products employ ASTM A36 steel plates, including bridge construction, vessels/tanks and pipes. According to the ASME XII, *the Rules for Construction and Continued Service of Transport Tanks*, ASTM steel

can be used as vessel shell material, one of which is pressure vessel transport tanks (Rodríguez-Prieto, Camacho, et al., 2021; Rodríguez-Prieto, Frigione, et al., 2021).

Pressure vessels have extra work to withstand thermal or non-thermal loads. Loads cause failure in pressure vessels (Haunstetter et al., 2020; Houška et al., 2022; Larrea-Wachtendorff et al., 2022), so engineers must analyze the failure of a material. By giving a load to the material, the effect of giving a load to the material being tested (Apriansyah et al., 2021). Pressure vessel failures can be grouped into four main categories, namely material (Rodríguez-Prieto, Camacho, et al., 2021; Rodríguez-Prieto, Frigione, et al., 2021), design (Regassa et al., 2022), fabrication (Liang et al., 2023) and service (Rodríguez-Prieto et al., 2022) which explain why failures occur. Failure can

CONTACT Muhammad Imam Ammarullah  imamammarullah@gmail.com  Department of Mechanical Engineering, Faculty of Engineering, Universitas Diponegoro, Semarang 50275, Central Java, Indonesia

© 2024 The Author(s). Published by Informa UK Limited, trading as Taylor & Francis Group

This is an Open Access article distributed under the terms of the Creative Commons Attribution License (<http://creativecommons.org/licenses/by/4.0/>), which permits unrestricted use, distribution, and reproduction in any medium, provided the original work is properly cited. The terms on which this article has been published allow the posting of the Accepted Manuscript in a repository by the author(s) or with their consent.

also be grouped into types of failure, namely elastic deformation, excessive plastic deformation, brittle fracture, stress rupture, plastic instability, high strain, stress corrosion and corrosion fatigue which describe how failure occurs (Ammarullah et al., 2022; Baigonakova et al., 2022; Frenelus et al., 2022; Nikulin et al., 2022; Yazdanpanah et al., 2021).

When transport tanks cross the road, pressure vessels will receive loads including shock loads which are influenced by road conditions, internal fluid loads and wind loads so the toughness and fatigue resistance of the vessels are very important to analyze (Chandra, Mataram, et al., 2019; Chandra, Sianturi, et al., 2019). The mechanical properties of transport tank materials that are important to analyze due to these problems include toughness and fatigue resistance. Material toughness is the material's ability to absorb energy before a fracture occurs (Waqas et al., 2019), while fatigue failure is a failure of the material due to cyclic or repetitive loading (Chandra, Mataram, et al., 2019; Chandra, Sianturi, et al., 2019). The studies of fatigue and crack behavior on pressure vessels for liquid petroleum gas (LPG) transport tanks are important to minimize the possibility of LPG transportation tank leaks, where leaks can have serious impacts on the environment and health, including air pollution and respiratory problems, damage to water and soil ecosystems, the potential to trigger explosions and fires and even cause death.

The analysis of fatigue and crack behavior using characterization in bending and impact tests is important for understanding material behavior, ensuring quality control, optimizing product design and complying with regulatory requirements. Several studies have been conducted to analyze the behavior of materials under different loading conditions. For example, one study analyzed the effect of stress concentration on the bending fatigue performance of gear steel using bending fatigue tests (Xing et al., 2019). Another study investigated the crack growth behaviors and mechanical properties degradation during gear bending fatigue using bending fatigue tests (Lin et al., 2019). Additionally, a study characterized the deformation field around a fatigue crack tip in the presence of significant plastic deformation using bending fatigue tests (Zhang et al., 2023). Another study conducted a fatigue test on the failure mode of flange shafts and characterized the propagation characteristics of the initial crack at the junction between the shaft using impact tests (Xu et al., 2022). These studies demonstrate the importance of using characterization in bending and impact tests to analyze the

fatigue and crack behavior of materials and components (Vasudevan & Sadananda, 2001).

The analysis of temperature in the fatigue and crack behavior on Pressure Vessels for LPG Transport tanks still limited, especially in the ASTM A36 steel material. Investigation of the two mechanical properties is important to study so that they can be used as a reference for the selection of welded construction steel materials for transport tanks. Also, it is brings beneficial to preventing environmental and health problems due to LPG transport tank leaks. From the explanation above, impact testing is required by providing shock loading and fatigue testing by continuously dynamic loading on pressure vessel steel (Halim et al., 2019; Pantazopoulos, 2019; Pratiwi et al., 2018). So, this study evaluation of impact test for without welded and welded joints with temperature and angle variations.

2. Materials and methods

2.1. Impact testing of the Charpy V-Notch method

This test was carried out in the Engineering Materials Laboratory, majoring in Mechanical Engineering, Sriwijaya University, Indralaya campus using a Charpy Impact Testing Machine type CI-30 with the JIS B7722 testing standard as shown in Figure 1. Figure 1(a) shows the schematic of the experimental method for impact testing, and Figure 1(b,c) shows the details of the specimen for the without welded and welded specimens. The welded process in this study following the Zhan et al. (2020), where potential energy retained at the lifting angle α of the pendulum (J), the position of the energy held at the swing angle θ of the pendulum (J), pendulum mass (25.68 kg), the distance from the center of the pendulum axis to the center of gravity (0.6490 m), pendulum lifting angle (146.5°), and Swing angle after the pendulum hits the specimen ($^\circ$) (Riyanto et al., 2022). The impact specimens used were based on the JIS Z 2202 standard.

In impact testing, the energy to break the specimen based on the angle formed by the pendulum (Galeja et al., 2020; Lascano et al., 2019; Zidan et al., 2019) is calculated through Equations (1)–(3). Where E_1 is potential energy retained at the lifting angle α of the pendulum (J), E_2 is the position of the energy held at the swing angle θ of the pendulum (J), P is pendulum mass (25.68 kg), D is the distance from the center of the pendulum axis to the center of gravity (0.6490 m), α is pendulum lifting angle

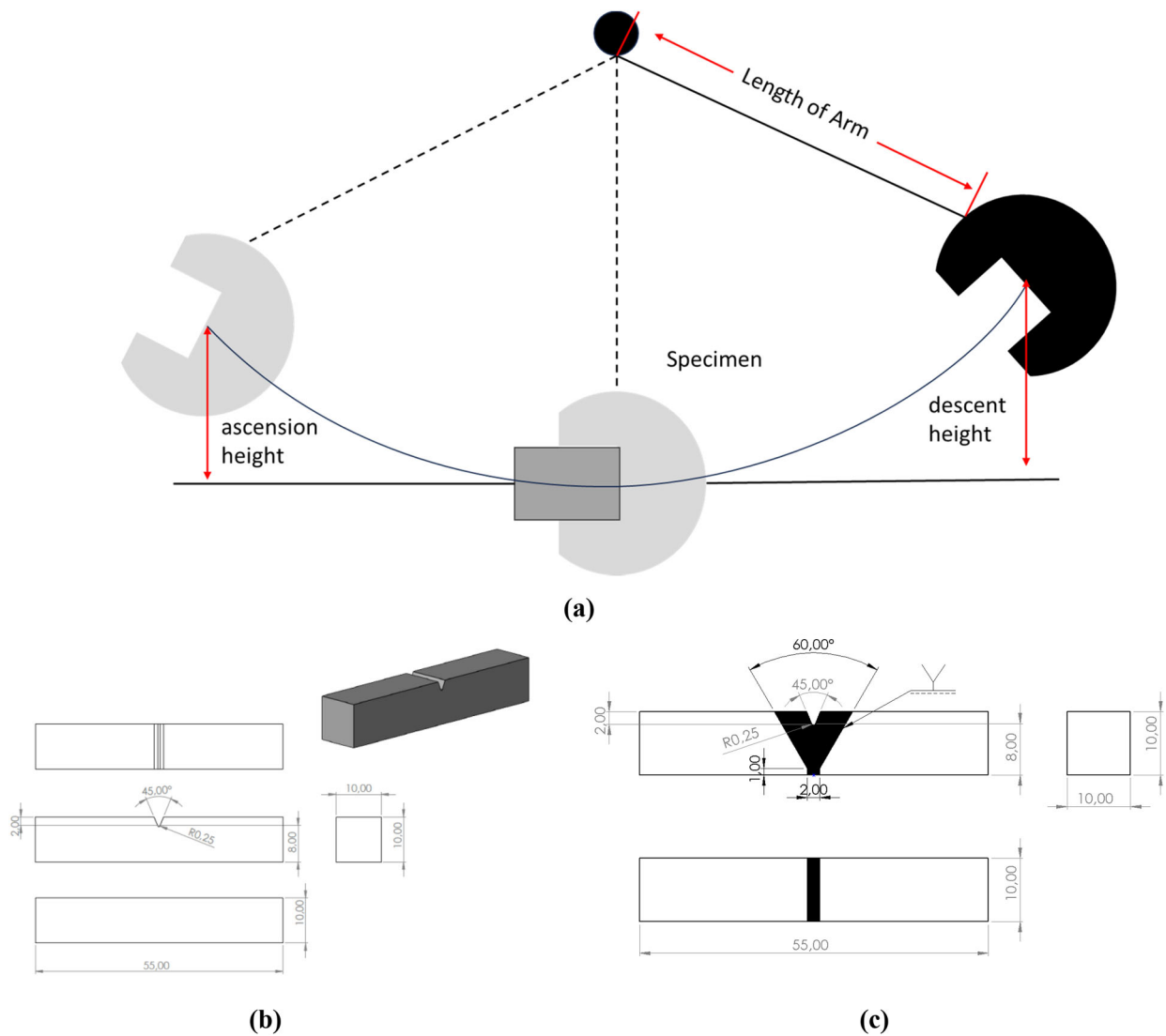


Figure 1. The schematic of (a) impact testing using Charpy V-Notch and The impact specimen JIS Z 2202: (b) without welded and (c) welded.

(146.5°) and θ is swing angle after the pendulum hits the specimen ($^\circ$).

$$E = E_1 - E_2 \quad (1)$$

$$E_1 = P (D - D \cos \alpha) \quad (2)$$

$$E_2 = P (D - D \cos \theta) \quad (3)$$

2.2. Fatigue testing with the repeated bending method

Fatigue testing was carried out using a Torsion and Bending Fatigue Machine with the test standard used being JIS Z 2273. Fatigue testing steps in this research follow research conducted by Firdaus et al. (2019). The fatigue specimen used the JIS Z 2273 standard as shown in Figure 2.

2.3. Determination of fatigue testing loading

The loading in the fatigue test can be predicted by calculating the bending stress whose value must be less than the yield strength value, in this case, the stress that occurs is still in an elastic condition (Chandra & Lestari, 2021). The composition and the mechanical properties of the ASTM 36 for this study as shown in Tables 1 and 2. Based on the yield strength value of ASTM A36 steel is 245 MPa, so the bending stress for fatigue testing must be less than 245 MPa.

In this study, the specimen was tested with applied the angle load in variation of the temperature at 0, 10 and 27°C . The selection of the variation temperature based on the working temperature conditions of LPG in the pressure vessel (Yukawa, 1990). The experiment was three repetitions to get the best result and the average data from the repetitions will be analyzed (Table 3).

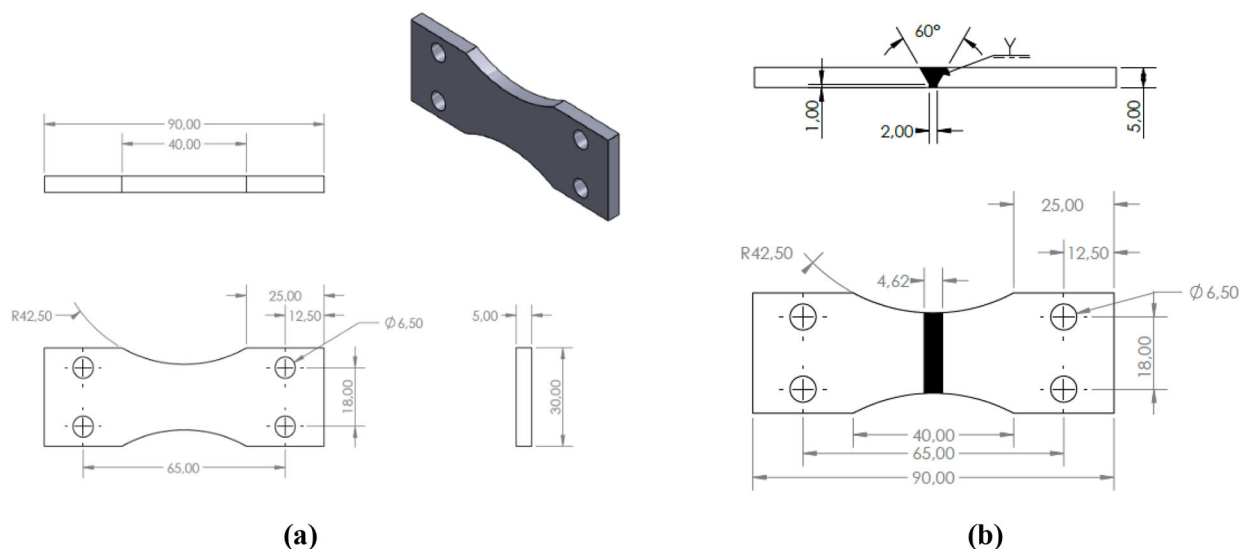


Figure 2. Fatigue Specimen JIS Z 2273: (a) without welded and (b) welded.

Table 1. ASTM A36 Steel chemical composition (% weight) (Surojo et al., 2021).

Composition	C	Si	Mn	P	S
(%)	0.2	0.24	1.067	0.025	0.024

Table 2. ASTM A36 steel mechanical properties (Preedawiphat et al., 2020).

Mechanical properties	Symbol	Value
Yield strength (MPa)	σ_y	245–300
Tensile strength (MPa)	σ_t	420–440
Elongation (%)	e	27–30

Table 3. Fatigue loading test with repeated bending method on ASTM A36 steel.

Angle load	Bending moment (N-mm)	Stress (MPa)
11	13,075.53	156.93
12	14,383.08	172.62
13	15,690.64	188.31
14	16,998.19	204.01

2.4. Visual observation

On visual observation of ASTM A36 steel, the fracture surface will be analyzed. It aims to see the types of fractures that occur and the crack propagation on the surface of the specimen marked by the presence of benchmarks, and then to compare the differences in the fracture surface on ASTM A36 steel specimens resulting from impact testing and fatigue testing (Chandra, Mataram, et al., 2019; Chandra, Sianturi, et al., 2019).

2.5. Metallographic examination

In the metallographic examination, the microstructure of ASTM A36 steel will be observed and analyzed to determine the phases formed due to heat

Table 4. Impact test results for without welded and welded joints.

Temperature (°C)	Welded			Without welded		
	α (°)	β (°)	Energy (J)	α (°)	β (°)	Energy (J)
0	146.5	118	6	146.5	100	9.67
10	146.5	115.5	8.2	146.5	85	11.8
27	146.5	110	9.9	146.5	70	17.28

treatment (Chandra et al., 2021). This comprehensive metallographic examination encompasses a detailed microstructural analysis of key components, including the base metal, Heat-affected Zone (HAZ), weld metal, and fusion lines on ASTM A36 steel. Utilizing an optical microscope with a magnification of 450x, the metallographic process is initiated following thorough specimen preparation procedures such as sanding and polishing. Subsequently, 3% Nital (NH₃) etching material is employed for the etching process. Post-etching, the specimens undergo photographic documentation at a magnification of 450x, utilizing an optical microscope within the metallurgical laboratory.

3. Results and discussion

3.1. Impact testing results

Impact test results for both conditions, namely for specimens with welded joints and without welds are shown in Table 4. Each test specimen for both conditions was tested at 0, 10 and 27 °C. The temperature is important to analysis in the working temperature conditions to detect the fatigue and crack behavior for reduce the potential of failure.

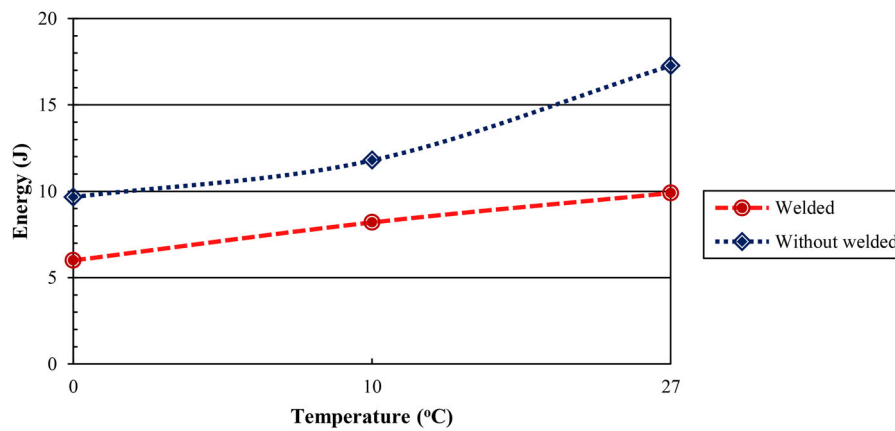


Figure 3. Impact testing curve.

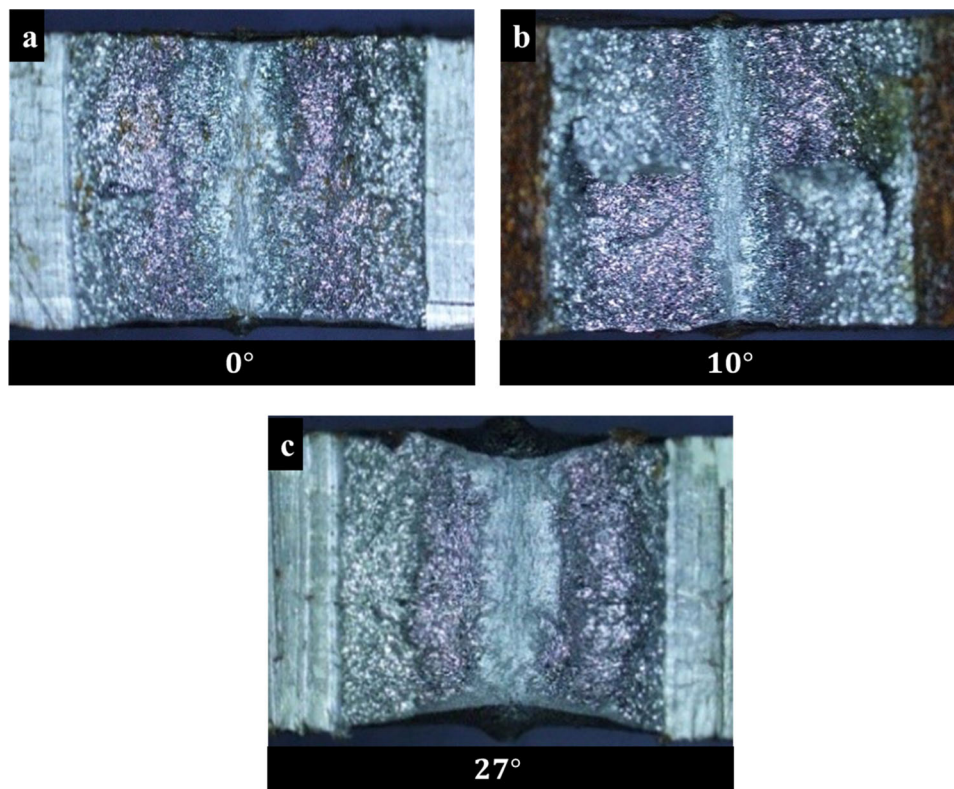


Figure 4. Condition of broken surface specimens of impact welded at a temperature of: (a) 0°C, (b) 10°C and (c) 27°C.

The results of the impact load test for both conditions without welding and with welded joints in Table 4 show that the value of the impact energy decreases as the operating temperature decreases. Decreasing the temperature causes the level of ductility to decrease then it will become more brittle so that the required impact energy also decreases (Perez et al., 2022; Salakhov et al., 2021; Williams & Boyer, 2020). The impact test specimen curve with welding shows a trend below the curve without welding, this is because the weld specimen shows weakness due to welding defects, and imperfections in the weld which have an impact on weakening the

metal (Luo et al., 2020; Niessen et al., 2020; Xue et al., 2022) as shown in Figure 3.

3.2. Impact testing fracture surface

Figure 4 shows the fracture characteristics for the impact test specimens tested for welding. It can be seen that the fracture surface at a low temperature of 0°C is hairy and flatter which indicates a brittle fracture, while the higher the temperature at 10°C and 27°C the broken surface looks smoother and there is an uneven surface. This is consistent with the impact energy which will decrease for lower

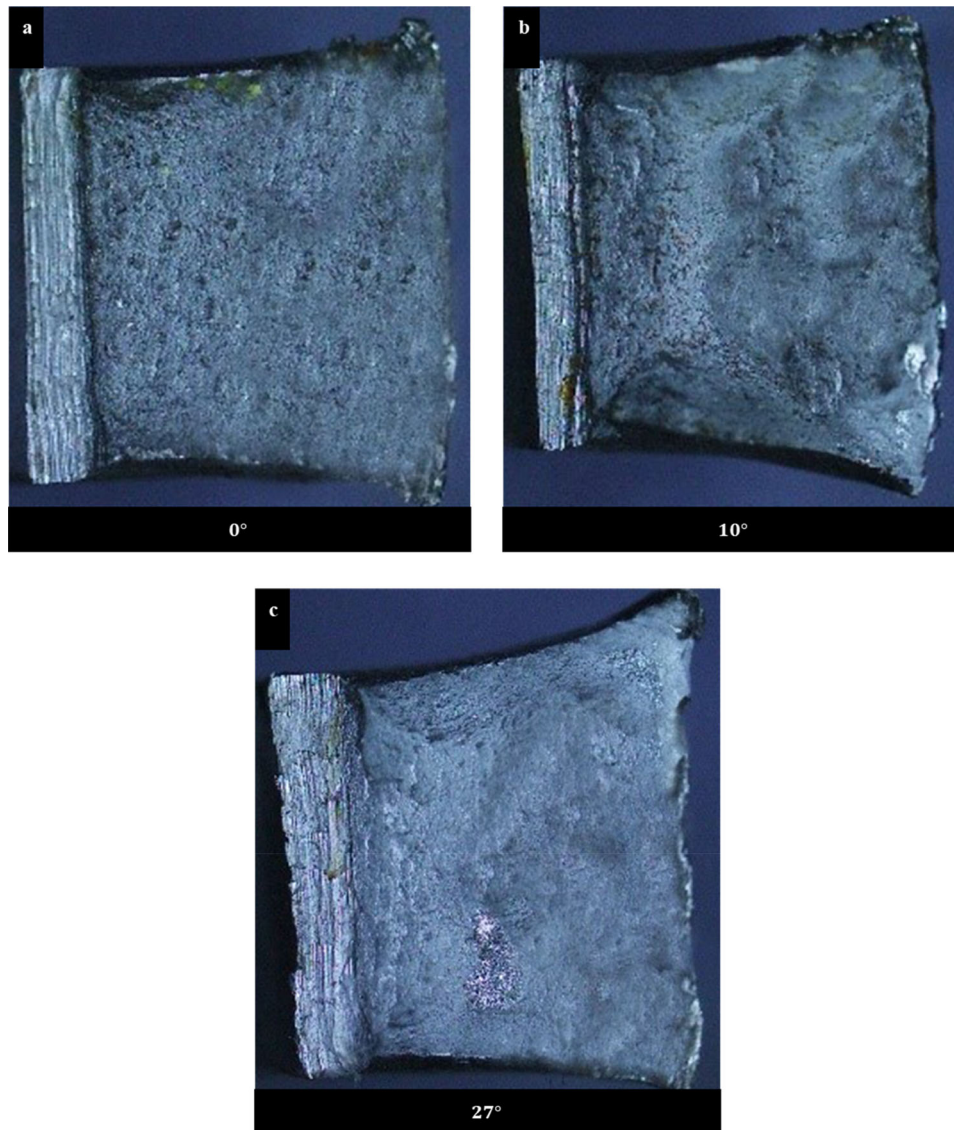


Figure 5. Condition of broken surface specimens of impact without welded at a temperature of: (a) 0°C, (b) 10°C and (c) 27°C.

temperatures compared to higher temperatures. Porosity is more evenly distributed for lower temperatures due to the impact of the welding process (Abidi et al., 2023).

In the non-welded impact test specimens, the fracture surface characteristics for temperatures of 0, 10 and 27°C did not show a significant difference. This is because there is no effect of welding heat that can change the microstructure in the heat-affected area (Chandra et al., 2018). This condition is shown in Figure 5.

3.3. Fatigue test results

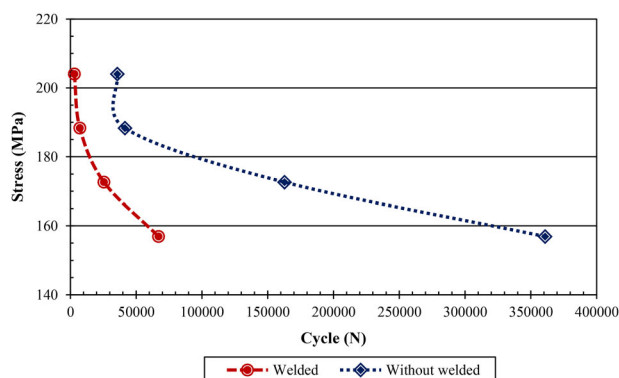
Fatigue testing was carried out on repeated bending fatigue testing machines with angle variations of 10°, 11°, 12° and 13°. The stress ratio applied was $R = 0$.

Tests were carried out for test specimens that were either subjected to heat treatment in the form of welding or without welding. The test results are shown in Table 5. The fracture cycle of the test specimens with welded joints was lower than those without welds. From the results, it is shown that the fatigue life of the test specimens which are welded is lower than that which is not welded. The greater the bending angle, the smaller the fracture cycle (Macek et al., 2021; Shi et al., 2022; Sun et al., 2021). This is because the working stress that occurs is directly proportional to the angle given in the fatigue test (Chen et al., 2022; Gan et al., 2021; Yang et al., 2022).

The fractured life results for both welded and non-welded conditions are shown in the relationship between the stress and cycle curves as shown in Figure 6. The S-N curve shows that the fatigue life of

Table 5. Impact test results for welded and without welded joints.

Angle load (°)	Welded				Without welded			
	Time (s)	Stress repeat (rps)	Cycle (N)	Stress (MPa)	Time (s)	Stress repeat (rps)	Cycle (N)	Stress (MPa)
10	1343	50	67,150	156.93	7216	50	360,800	156.93
11	512	50	25,600	172.62	3256	50	162,800	172.62
12	146	50	7300	188.31	831	50	41,550	188.31
13	62	50	3100	204.01	715	50	35,750	204.01

**Figure 6.** S-N curve for fatigue testing of welded and without-welded specimens.

the test specimens that were welded was lower than that of the test specimens without welds. In the test specimens that were welded, all four specimens experienced fracture before 100,000 cycles, while the test specimens without welds varied more. Two variations of angles 10° and 11° fracture before 100,000 cycles, while angles 12° and 13° test specimens experience longer fractures above 100,000 cycles and some even close to 400,000 cycles.

3.4. Fractured surface in fatigue testing

The fracture surface characteristics of the test specimens that were welded with various test angles of 10° , 11° , 12° and 13° are shown in Figure 7. The fracture surface consists of stages, namely the crack initiation stage, the crack propagation stage, and the final fracture stage (Hou et al., 2016; Liu & Pons, 2018; Xiao et al., 2021). The fatigue fracture surface is characterized by a flat and smooth surface, while the final fracture, which is a static fracture, is characterized by a plastically deformed fracture shape. The initial crack begins in a weak area of the weld defect which can trigger an increase in stress in that area (Kubit et al., 2020). Examination of the fatigue fracture surface in the form of visual observations is not very clear to get the characteristics of a fatigue fracture in the form of beach marks. The absence of beach marks in the fatigue fracture surface visual observations is due to the test being carried out at a stress ratio condition equal to zero ($R=0$). Beach marks, which are

characteristic features of fatigue fractures, appear clearer when the test is carried out at $R=1$. At $R=1$, the fatigue fracture surface exhibits distinct beach marks, which are indicative of the crack growth direction and can provide valuable information about the fatigue process. However, the absence of beach marks at $R=0$ does not diminish the evidence of a fatigue fracture surface with the indications described previously (Braun et al., 2022; Macek et al., 2020).

3.5. Metallographic results

Metallographic examination in the form of examining the microstructure of pressure vessel materials, especially in the weld area, needs to be observed to what extent the effect of welding heat on steel is commonly used for pressure vessel needs, especially in areas affected by heat. The microstructure formed is in the form of ferrite and pearlite phases, where pearlite is a layer between ferrite and cementite (Chandra et al., 2020) as shown in Figure 8. In the filler metal area, the pearlite fraction appears to be more than the ferrite phase. This shows that the type of filler metal used in welding uses steel with a higher composition. This is because the carbon content can increase the cementite Fe_3C fraction so that it adds more pearlite fractions (Banis et al., 2019; Handoko et al., 2018; Oliveira Anício Costa et al., 2022). In the weld fusion area, it shows martensite and pearlite fractions, while in the HAZ area, it can see the difference in grain size compared to the parent metal or base metal. Enlarged grains make the metal decrease in strength compared to fine metal grains (Weidner et al., 2019; Yang et al., 2019; Yuan et al., 2018; Zienert et al., 2021).

4. Conclusions

In conclusion, the study provides insights into the fatigue and crack behavior of ASTM A36 steel under different testing conditions that would lead to preventing environmental and health problems due to LPG transport tank leaks. Impact testing revealed a decrease in impact energy with decreasing temperatures, particularly pronounced in welded specimens.

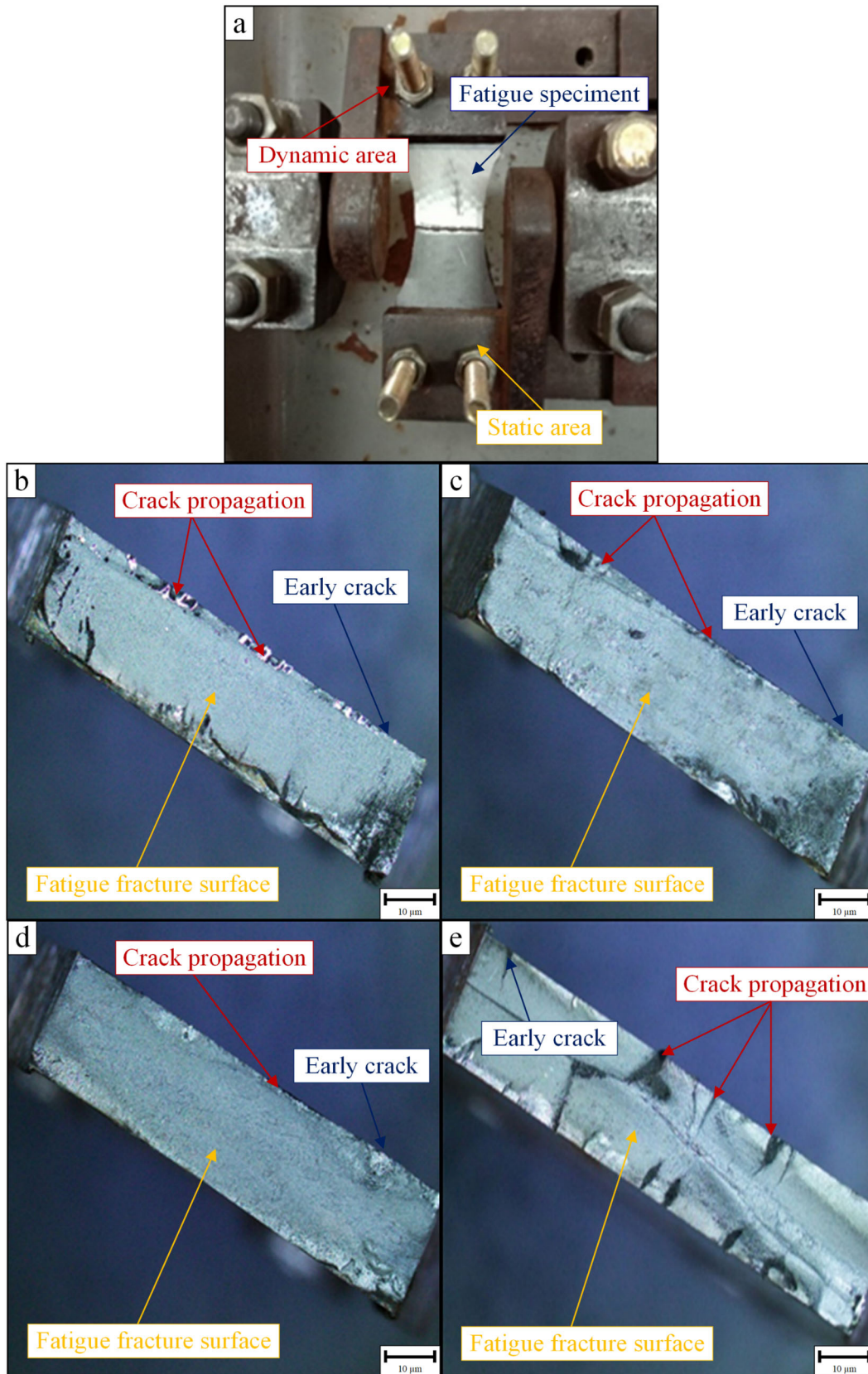


Figure 7. (a) Specimen conditions of fatigue weld joints before being observed under a microscope; Surface condition with angle loading of (b) 10°, (c) 11°, (d) 12° and (e) 13°.

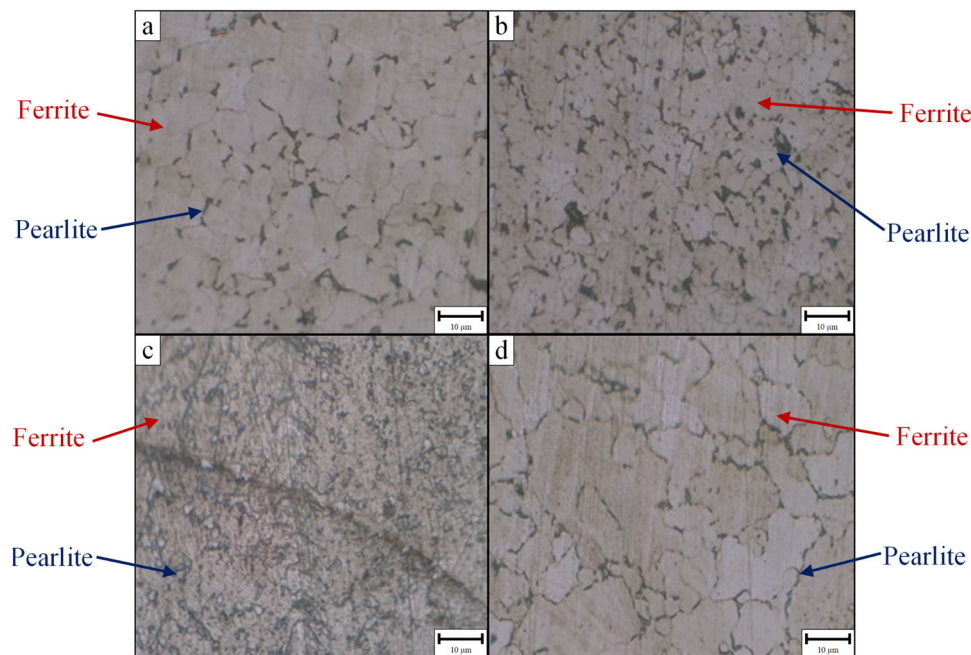


Figure 8. 450x magnification: (a) Metal base, (b) Weld Metal, (c) Fusion Line and (d) HAZ.

The investigation revealed a shorter fatigue life for welded specimens compared to non-welded counterparts, as illustrated by the S-N curve. Visual observations of fracture surfaces indicated variations in characteristics, particularly in welded specimens, affected by welding defects. The metallographic examination underscored the necessity for understanding the varied material behavior under dissimilar loading conditions, a crucial aspect for effective application in pressure vessel transport tanks.

Institutional Review Board statement

Not applicable.

Informed consent statement

Not applicable.

Consent for publication

All authors consent for the publication of this manuscript.

Acknowledgments

The authors gratefully thank the author's respective institution for their strong support in this study.

Disclosure statement

The authors declare no conflict of interest.

Author contribution

Hendri Chandra: Conceptualization, Methodology, Supervision and Funding Acquisition.

Muhammad Imam Ammarullah: Software, Validation, Writing – review and editing, Visualization and Project administration.

M. Marwani: Software, Validation and Formal analysis.

E. Ellyanie: Software, Validation and Formal analysis.

W. Warizal: Investigation and Resources.

Dimas Aditya: Formal analysis, Investigation and Writing – original draft preparation.

Diah Kusuma Pratiwi: Conceptualization, Methodology and Supervision.

Nurhabibah Paramitha Eka Utami: Conceptualization, Methodology and Supervision.

Funding

The research was funded by Universitas Sriwijaya.

ORCID

Hendri Chandra <http://orcid.org/0000-0001-9378-2299>

Muhammad Imam Ammarullah <http://orcid.org/0000-0002-8845-7202>

M. Marwani <http://orcid.org/0000-0002-3608-7772>

Diah Kusuma Pratiwi <http://orcid.org/0000-0003-4457-9803>

Nurhabibah Paramitha Eka Utami <http://orcid.org/0000-0002-4533-1204>

Data availability statement

The necessary data used in the manuscript are already present in the manuscript.

References

- Abidi, M. H., Moiduddin, K., Siddiquee, A. N., Mian, S. H., & Mohammed, M. K. (2023). Development of aluminium metal foams via friction stir processing by utilizing MgCO₃ precursor. *Coatings*, *13*(1), 162. <https://doi.org/10.3390/coatings13010162>
- Ammarullah, M., Santoso, G., Sugiharto, S., Supriyono, T., Wibowo, D., Kurdi, O., Tauviqirrahman, M., & Jamari, J. (2022). Minimizing risk of failure from ceramic-on-ceramic total hip prosthesis by selecting ceramic materials based on tresca stress. *Sustainability*, *14*(20), 13413. <https://doi.org/10.3390/su142013413>
- Apriansyah, A., Chandra, H., Pratiwi, D. K., & Firdaus, A. (2021). Fatigue failure on drilling pipe thread: A case study on drill pipe Ss105. *Indonesian Journal of Engineering and Science*, *1*(1), 011–019. <https://doi.org/10.51630/ijes.v1i1.6>
- Baigonakova, G., Marchenko, E., Kovaleva, M., & Vorozhtsov, A. (2022). Influence of wire geometry on the mechanical behavior of the TiNi esign. *Metals (Basel)*, *12*(7), 1131. <https://doi.org/10.3390/met12071131>
- Banis, A., Hernandez Duran, E., Bliznuk, V., Sabirov, I., Petrov, R. H., & Papaefthymiou, S. (2019). The effect of ultra-fast heating on the microstructure, grain size and texture evolution of a commercial low-C, medium-Mn DP steel. *Metals (Basel)*, *9*(8), 877. <https://doi.org/10.3390/met9080877>
- Braun, M., Fischer, C., Baumgartner, J., Hecht, M., & Varfolomeev, I. (2022). Fatigue crack initiation and propagation relation of notched specimens with welded joint characteristics. *Metals (Basel)*, *12*(4), 615. <https://doi.org/10.3390/met12040615>
- Chandra, H., Dahlan, H., Paramitha Eka Utami, N., Tito, A., & Warizal. (2021). Increase the toughness of material of construction using heat treatment. *IOP Conference Series: Earth and Environmental Science*, *810*(1), 012015. <https://doi.org/10.1088/1755-1315/810/1/012015>
- Chandra, H., & Lestari, V. (2021). Analysis of the effect of stop drilled hole diameter variation on fatigue resistance in medium carbon steel DIN HQ 705. *IOP Conference Series: Earth and Environmental Science*, *810*(1), 012016. <https://doi.org/10.1088/1755-1315/810/1/012016>
- Chandra, H., Mataram, A., & Utami, N. (2019). The characterization of mechanical property and fatigue life of betel-falm fiber composite as environmentally-friendly material. *IOP Conference Series: Materials Science and Engineering*, *620*(1), 012119. <https://doi.org/10.1088/1757-899X/620/1/012119>
- Chandra, H., Pratiwi, D. K., & Zahir, M. (2018). High-temperature quality of accelerated spheroidization on SUP9 leaf spring to enhance machinability. *Heliyon*, *4*(12), e01076. <https://doi.org/10.1016/j.heliyon.2018.e01076>
- Chandra, H., Falisa, & Harnani. (2020). Geochemical studies of claystone based on analysis of scanning electron microscope (SEM), Talangsawah, Merapi District and surroundings of Lahat Regency, South Sumatra. *Journal of Physics: Conference Series*, *1500*(1), 012079. <https://doi.org/10.1088/1742-6596/1500/1/012079>
- Chandra, H., Sianturi, B., & Nukman. (2019). Analysis of fatigue life and crack propagation characterization of gray cast iron under normalizing process. *Journal of Physics: Conference Series*, *1198*(3), 032006. <https://doi.org/10.1088/1742-6596/1198/3/032006>
- Chandra, H. (2019). Mechanical fracture characterization of rice kernel under milling process. *Journal of Physics: Conference Series*, *1198*(4), 042011. <https://doi.org/10.1088/1742-6596/1198/4/042011>
- Chen, C., Li, Z., Xu, C., Zhu, Z., & Zou, S. (2022). Variation of fracture toughness with biaxial load and T-stress under mode I condition. *Applied Sciences*, *12*(18), 9319. <https://doi.org/10.3390/app12189319>
- Firdaus, M. S., Yani, I., Arifin, A., Arifta, P., Surya, I., & Nukman. (2019). The effect of heat treatment on fatigue testing of aluminum cans. *Journal of Physics: Conference Series*, *1198*(7), 072002. <https://doi.org/10.1088/1742-6596/1198/7/072002>
- Frenelus, W., Peng, H., & Zhang, J. (2022). Creep behavior of rocks and its application to the long-term stability of deep rock tunnels. *Applied Sciences*, *12*(17), 8451. <https://doi.org/10.3390/app12178451>
- Galeja, M., Hejna, A., Kosmela, P., & Kulawik, A. (2020). Static and dynamic mechanical properties of 3D printed ABS as a function of raster angle. *Materials (Basel, Switzerland)*, *13*(2), 297. <https://doi.org/10.3390/ma13020297>
- Gan, J., Gao, Z., Wang, Y., Wang, Z., & Wu, W. (2021). Small-scale experimental investigation of fatigue performance improvement of ship hatch corner with shot peening treatments by considering residual stress relaxation. *Journal of Marine Science and Engineering*, *9*(4), 419. <https://doi.org/10.3390/jmse9040419>
- Halim, M., Chandra, H., Pratiwi, D. K., & Zahir, M. (2019). Sustainable development of lubricator to optimization process of lubrication in wire rope sling. *Journal of Physics: Conference Series*, *1198*(4), 042005. <https://doi.org/10.1088/1742-6596/1198/4/042005>
- Handoko, W., Pahlevani, F., & Sahajwalla, V. (2018). Enhancing corrosion resistance and hardness properties of carbon steel through modification of microstructure. *Materials (Basel, Switzerland)*, *11*(12), 2404. <https://doi.org/10.3390/ma11122404>
- Haunstetter, J., Krüger, M., & Zunft, S. (2020). Experimental studies on thermal performance and thermo-structural stability of steelmaking slag as inventory material for thermal energy storage. *Applied Sciences*, *10*(3), 931. <https://doi.org/10.3390/app10030931>
- Hou, J. P., Wang, Q., Yang, H. J., Wu, X. M., Li, C. H., Zhang, Z. F., & Li, X. W. (2016). Fatigue and fracture behavior of a cold-drawn commercially pure aluminum wire. *Materials (Basel, Switzerland)*, *9*(9), 764. <https://doi.org/10.3390/ma9090764>
- Houška, M., Silva, F. V. M., Buckow, R., Terefe, N. S., Tonello, C., & Evelyn. (2022). High pressure processing applications in plant foods. *Foods (Basel, Switzerland)*, *11*(2), 223. <https://doi.org/10.3390/foods11020223>
- Kim, J., Kim, J., Kang, S., & Chun, K. (2020). Laser welding of ASTM A553-1 (9% nickel steel) (PART I: Penetration shape by bead on plate). *Metals (Basel)*, *10*(4), 484. <https://doi.org/10.3390/met10040484>
- Kubit, A., Drabczyk, M., Trzepieciniski, T., Bochnowski, W., Kašćák, L., & Slota, J. (2020). Fatigue life assessment of refill friction stir spot welded clad 7075-T6 aluminium

- alloy joints. *Metals (Basel)*, 10(5), 633. <https://doi.org/10.3390/met10050633>
- Larrea-Wachtendorff, D., Del Grosso, V., & Ferrari, G. (2022). Evaluation of the physical stability of starch-based hydrogels produced by high-pressure processing (HPP). *Gels (Basel, Switzerland)*, 8(3), 152. <https://doi.org/10.3390/gels8030152>
- Lascano, D., Quiles-Carrillo, L., Balart, R., Boronat, T., & Montanes, N. (2019). Toughened poly(lactic acid)—PLA formulations by binary blends with poly(butylene succinate-co-adipate)—PBSA and their shape memory behaviour. *Materials (Basel, Switzerland)*, 12(4), 622. <https://doi.org/10.3390/ma12040622>
- Liang, J., Liu, L., Qin, Z., Zhao, X., Li, Z., Emmanuel, U., & Feng, J. (2023). Experimental study of curing temperature effect on mechanical performance of carbon fiber composites with application to filament winding pressure vessel design. *Polymers*, 15(4), 982. <https://doi.org/10.3390/polym15040982>
- Lin, B., Alshammrei, S., Wigger, T., & Tong, J. (2019). Characterisation of fatigue crack tip field in the presence of significant plasticity. *Theoretical and Applied Fracture Mechanics*, 103, 102298. <https://doi.org/10.1016/j.tafmec.2019.102298>
- Liu, D., & Pons, D. (2018). Crack propagation mechanisms for creep fatigue: A consolidated explanation of fundamental behaviours from initiation to failure. *Metals (Basel)*, 8(8), 623. <https://doi.org/10.3390/met8080623>
- Luo, Y., Gu, W., Peng, W., Jin, Q., Qin, Q., & Yi, C. (2020). A study on microstructure, residual stresses and stress corrosion cracking of repair welding on 304 stainless steel: Part I-effects of heat input. *Materials (Basel, Switzerland)*, 13(10), 2416. <https://doi.org/10.3390/ma13102416>
- Macek, W., Branco, R., Costa, J. D., & Tremback, J. (2021). Fracture surface behavior of 34CrNiMo6 high-strength steel bars with blind holes under bending-torsion fatigue. *Materials (Basel, Switzerland)*, 15(1), 80. <https://doi.org/10.3390/ma15010080>
- Macek, W., Branco, R., Szala, M., Marciniak, Z., Ulewicz, R., Sczygiol, N., & Kardasz, P. (2020). Profile and areal surface parameters for fatigue fracture characterisation. *Materials (Basel, Switzerland)*, 13(17), 3691. <https://doi.org/10.3390/MA13173691>
- Niessen, B., Schumacher, E., Lueg-Althoff, J., Bellmann, J., Böhme, M., Böhm, S., Tekkaya, A. E., Beyer, E., Leyens, C., Wagner, M. F. X., & Groche, P. (2020). Interface formation during collision welding of aluminum. *Metals (Basel)*, 10(9), 1202. <https://doi.org/10.3390/met10091202>
- Nikulin, S. A., Rogachev, S. O., Belov, V. A., Zadorozhnyy, M. Y., Shplis, N. V., & Skripalenko, M. M. (2022). Effect of prolonged thermal exposure on low-cycle bending fatigue resistance of low-carbon steel. *Metals (Basel)*, 12(2), 281. <https://doi.org/10.3390/met12020281>
- Oliveira Anício Costa, I. M., Batková, M., Batko, I., Benabou, A., Mesplont, C., & Vogt, J. B. (2022). The influence of microstructure on the electromagnetic behavior of carbon steel wires. *Crystals*, 12(5), 576. <https://doi.org/10.3390/cryst12050576>
- Pantazopoulos, G. (2019). A short review on fracture mechanisms of mechanical components operated under industrial process conditions: Fractographic analysis and selected prevention strategies. *Metals (Basel)*, 9(2), 148. <https://doi.org/10.3390/met9020148>
- Perez, M., Akhavan-Safar, A., Carbas, R. J. C., Marques, E. A. S., Wenig, S., & da Silva, L. F. M. (2022). Loading rate and temperature interaction effects on the mode I fracture response of a ductile polyurethane adhesive used in the automotive industry. *Materials (Basel, Switzerland)*, 15(24), 8948. <https://doi.org/10.3390/ma15248948>
- Pratiwi, D. K., Chandra, H., Utami, N. P. E., Irawan, O., & Purba, A. N. (2018). Damage analysis of moldboard plow. Amin M, editor. *E3S Web of Conferences*, 68, 04004. <https://doi.org/10.1051/e3sconf/20186804004>
- Pratiwi, D. K., Arifin, A., Mardhi, A., Gunawan, & Afriansyah. (2023). Investigation of welding parameters of dissimilar weld of SS316 and ASTM A36 joint using a grey-based taguchi optimization approach. *Journal of Manufacturing and Materials Processing*, 7(1), 39. <https://doi.org/10.3390/jmmp7010039>
- Preedawiphat, P., Mahayotsanun, N., Sa-Ngoen, K., Noipitak, M., Tuengsook, P., Sucharitpawatskul, S., & Dohda, K. (2020). Mechanical investigations of ASTM A36 welded steels with stainless steel cladding. *Coatings*, 10(9), 844. <https://doi.org/10.3390/coatings10090844>
- Regassa, Y., Gari, J., & Lemu, H. G. (2022). Composite over-wrapped pressure vessel design optimization using numerical method. *Journal of Composites Science*, 6(8), 229. <https://doi.org/10.3390/jcs6080229>
- Riyanto, H., Sugito, S., & Fikri, A. (2022). Optimization of wire type and current welding on the strength of welding connection in two types of material testing via response surface methodology. *Engineering Solid Mechanics*, 10(4), 341–350. <https://doi.org/10.5267/j.esm.2022.6.004>
- Rodríguez-Prieto, A., Callejas, M., Primera, E., Lomonaco, G., & Camacho, A. M. (2022). Multicriteria analytical model for mechanical integrity prognostics of reactor pressure vessels manufactured from forged and rolled steels. *Mathematics*, 10(10), 1779. <https://doi.org/10.3390/math10101779>
- Rodríguez-Prieto, A., Camacho, A. M., Mendoza, C., Kickhofel, J., & Lomonaco, G. (2021). Evolution of standardized specifications on materials, manufacturing and in-service inspection of nuclear reactor vessels. *Sustainability*, 13(19), 10510. <https://doi.org/10.3390/su131910510>
- Rodríguez-Prieto, A., Frigione, M., Kickhofel, J., & Camacho, A. M. (2021). Analysis of the technological evolution of materials requirements included in reactor pressure vessel manufacturing codes. *Sustainability*, 13(10), 5498. <https://doi.org/10.3390/su13105498>
- Salakhov, I. I., Shaidullin, N. M., Chalykh, A. E., Matsko, M. A., Shapagin, A. V., Batyrshin, A. Z., Shandryuk, G. A., & Nifant'ev, I. E. (2021). Low-temperature mechanical properties of high-density and low-density polyethylene and their blends. *Polymers*, 13(11), 1821. <https://doi.org/10.3390/polym13111821>
- Shi, Z., Li, J., Zhang, X., Shang, C., & Cao, W. (2022). Influence mechanisms of inclusion types on rotating bending fatigue properties of SAE52100 bearing steel.

- Materials (Basel, Switzerland)*, 15(14), 5037. <https://doi.org/10.3390/ma15145037>
- Sun, F., Lv, L. T., Cheng, W., Zhang, J. L., Ba, D. C., Song, G. Q., & Lin, Z. (2021). Effect of loading angles and implant lengths on the static and fatigue fractures of dental implants. *Materials (Basel, Switzerland)*, 14(19), 5542. <https://doi.org/10.3390/ma14195542>
- Surojo, E., Gumilang, A. H., Triyono, T., Prabowo, A. R., Budiana, E. P., & Muhayat, N. (2021). Effect of water flow on underwater wet welded A36 steel. *Metals (Basel)*, 11(5), 682. <https://doi.org/10.3390/met11050682>
- Tamlich, A., Farhan, A., Fadhillah, T. A., Firs, T., Raja Ghazilla, R. A., Akhyar, Azwinur, & Syukran. (2022). Evaluation of welding distortion and hardness in the A36 steel plate joints using different cooling media. *Sustainability*, 14(3), 1405. <https://doi.org/10.3390/su14031405>
- Utami, N. P. E., & Chandra, H. (2017). Mechanical properties analysis of Al-9Zn-5Cu-4Mg cast alloy by T5 heat treatment. Iskandar I, Ismadji S, Agustina. *MATEC Web of Conferences*, 101, 01009. <https://doi.org/10.1051/matec-conf/201710101009>
- Vasudevan, A. K., & Sadananda, K. (2001). Analysis of fatigue crack growth under compression-compression loading. *International Journal of Fatigue*, 23, 365–374. [https://doi.org/10.1016/s0142-1123\(01\)00172-4](https://doi.org/10.1016/s0142-1123(01)00172-4)
- Waqas, A., Qin, X., Xiong, J., Zheng, C., & Wang, H. (2019). Analysis of ductile fracture obtained by charpy impact test of a steel structure created by robot-assisted GMAW-based additive manufacturing. *Metals (Basel)*, 9(11), 1208. <https://doi.org/10.3390/met9111208>
- Weidner, A., Ranglack-Klemm, Y., Zienert, T., Aneziris, C. G., & Biermann, H. (2019). Mechanical high-temperature properties and damage behavior of coarse-grained alumina refractory metal composites. *Materials (Basel, Switzerland)*, 12(23), 3927. <https://doi.org/10.3390/ma12233927>
- Williams, J. C., & Boyer, R. R. (2020). Opportunities and issues in the application of titanium alloys for aerospace components. *Metals (Basel)*, 10(6), 705. <https://doi.org/10.3390/met10060705>
- Xiao, P., Li, D., Zhao, G., & Liu, M. (2021). Experimental and numerical analysis of mode I fracture process of rock by semi-circular bend specimen. *Mathematics*, 9(15), 1769. <https://doi.org/10.3390/math9151769>
- Xing, Z., Wang, Z., Wang, H., & Shan, D. (2019). Bending fatigue behaviors analysis and fatigue life prediction of 20Cr2Ni4 gear steel with different stress concentrations near non-metallic inclusions. *Materials (Basel, Switzerland)*, 12(20), 3443. <https://doi.org/10.3390/ma12203443>
- Xu, Z., Cui, Y., Li, B., Liu, K., Shi, F., & Cao, P. (2022). Impact analysis of initial cracks' angle on fatigue failure of flange shafts. *Coatings*, 12(2), 276. <https://doi.org/10.3390/coatings12020276>
- Xue, F., He, D., & Zhou, H. (2022). Effect of ultrasonic vibration in friction stir welding of 2219 aluminum alloy: An effective model for predicting weld strength. *Metals (Basel)*, 12(7), 1101. <https://doi.org/10.3390/met12071101>
- Yang, D., Tang, S., Hu, Y., Nikitin, A., Wang, Q., Liu, Y., Li, L., He, C., Li, Y., Xu, B., & Wang, C. (2022). A novel model of ultrasonic fatigue test in pure bending. *Materials (Basel, Switzerland)*, 15(14), 4864. <https://doi.org/10.3390/ma15144864>
- Yang, Q., Xia, C., Deng, Y., Li, X., & Wang, H. (2019). Microstructure and mechanical properties of AlSi7Mg0.6 aluminum alloy fabricated by wire and arc additive manufacturing based on cold metal transfer (WAAM-CMT). *Materials (Basel, Switzerland)*, 12(16), 2525. <https://doi.org/10.3390/ma12162525>
- Yazdanpanah, A., Lago, M., Gennari, C., & Dabalà, M. (2021). Stress corrosion cracking probability of selective laser melted 316L austenitic stainless steel under the effect of grinding induced residual stresses. *Metals (Basel)*, 11(2), 327. <https://doi.org/10.3390/met11020327>
- Yuan, Q., Xu, G., Liu, S., Liu, M., Hu, H., & Li, G. (2018). Effect of rolling reduction on microstructure and property of ultrafine grained low-carbon steel processed by cryorolling martensite. *Metals (Basel)*, 8(7), 518. <https://doi.org/10.3390/met8070518>
- Yukawa, S. (1990). *Guidelines for pressure vessel safety assessment*. NIST special publication 780. National Institute of Standards and Technology
- Zhan, N., Hu, Z., & Zhang, X. (2020). Experimental investigation of fatigue crack growth behavior in banded structure of pipeline steel. *Metals (Basel)*, 10(9), 1193. <https://doi.org/10.3390/met10091193>
- Zhang, Y., Tang, Z., Zhao, L., Gong, B., Wang, G., & Li, Z. (2023). Effect of initial crack position on crack propagation behaviors of heavy-duty transmission gear. *Materials (Basel, Switzerland)*, 16(17), 5961. <https://doi.org/10.3390/ma16175961>
- Zidan, S., Silikas, N., Alhotan, A., Haider, J., & Yates, J. (2019). Investigating the mechanical properties of ZrO₂-impregnated PMMA nanocomposite for denture-based applications. *Materials (Basel, Switzerland)*, 12(8), 1344. <https://doi.org/10.3390/ma12081344>
- Zienert, T., Endler, D., Hubálková, J., Günay, G., Weidner, A., Biermann, H., Kraft, B., Wagner, S., & Aneziris, C. G. (2021). Synthesis of niobium-alumina composite aggregates and their application in coarse-grained refractory ceramic-metal castables. *Materials (Basel, Switzerland)*, 14(21), 6453. <https://doi.org/10.3390/ma14216453>